Article

Current Biology

STRIPAK Limits Stem Cell Differentiation of a WNT Signaling Center to Control Planarian Axis Scaling

Graphical Abstract

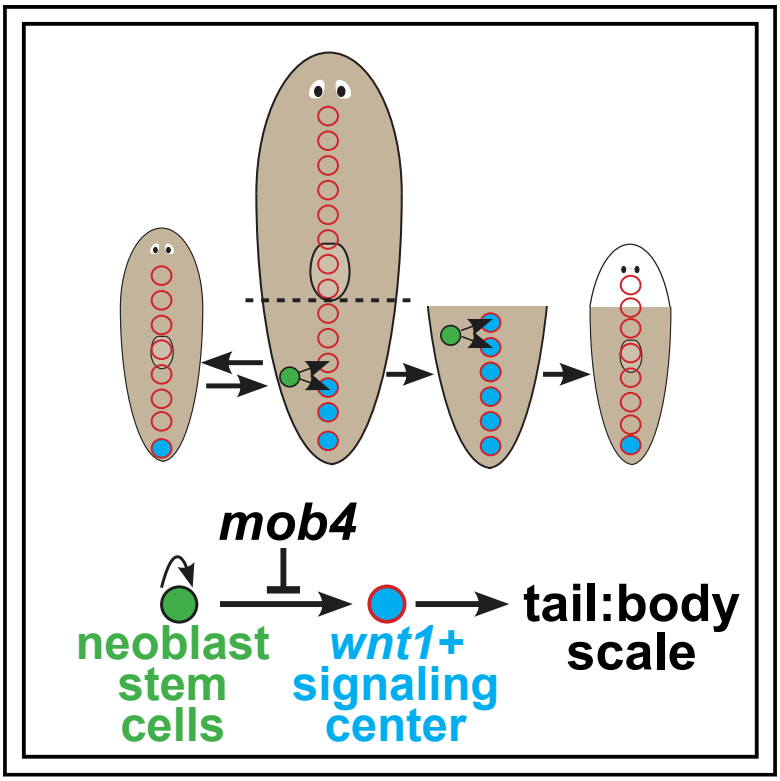

Highlights

- *mob4* of the STRIPAK complex limits body size in planarians
- *wnt1+* posterior signaling-center cells promote tail size during regeneration
- *mob4* limits differentiation of *wnt1+* pole cells from stem cells
- Production of specialized signaling cells regulates organ size in regeneration

Authors

Erik G. Schad, Christian P. Petersen

Correspondence

christian-p-petersen@northwestern.edu

In Brief

Planarians must scale the relative size of tissues to accomplish regeneration. Schad and Petersen identify the *mob4* and *striatin* components of the STRIPAK complex as negative regulators of tail size in planarians. STRIPAK acts by limiting stem cell differentiation of Wnt-expressing signaling-center cells that determine posterior scaling.

Schad & Petersen, 2020, Current Biology *30*, 254–263
January 20, 2020
https://doi.org/10.1016/j.cub.2019.11.068

CellPress

CellPress

Current Biology
Article

STRIPAK Limits Stem Cell Differentiation of a WNT Signaling Center to Control Planarian Axis Scaling

Erik G. Schad[1] and Christian P. Petersen[1,2,3,*]
[1]Department of Molecular Biosciences, Northwestern University, Evanston, IL 60208, USA
[2]Robert Lurie Comprehensive Cancer Center, Northwestern University, Evanston IL 60208, USA
[3]Lead Contact
*Correspondence: christian-p-petersen@northwestern.edu
https://doi.org/10.1016/j.cub.2019.11.068

SUMMARY

Regeneration involves regulating tissue proportionality across considerable size ranges through unknown mechanisms. In planarians, which scale reversibly over 40× through regeneration, we identify the Striatin-interacting phosphatase and kinase (STRIPAK) complex as a potent negative regulator of axis length. Inhibition of two proteins in the STRIPAK complex, *mob4* and *striatin*, dramatically increased posterior length, through expansion of a posterior *wnt1*+ signaling center within midline muscle cells. *wnt1* was required for tail expansion after *mob4* inhibition and dynamically reestablishes proportionality after amputation in normal animals, indicating STRIPAK represses Wnt signaling for scaling. Regulation of *wnt1* expansion was stem cell dependent, demonstrating that control of signaling-center production through stem cell differentiation underlies proportional growth in adult regenerative tissue.

INTRODUCTION

Proportional tissue scaling is fundamental to organismal form. Within species, the relative sizes of appendages or organs scale in stereotyped ways with respect to body size, for example arm span versus height in humans. Across species, modifications to organ proportionality can underlie morphological evolution [1]. Morphogens that enable communication across cell populations have been implicated in both size attainment and proportional scaling through growth. Examples include the Dpp gradient within *Drosophila* imaginal discs, the Bicoid gradient within the *Drosophila* syncytial blastoderm, or the dorsoventral BMP gradient of *Xenopus* and zebrafish embryos, all of which function over the range of ~10 to 100 s of microns [2–4]. However, it is unclear what mechanisms ensure proportional growth across the much larger scale of adult growth, which can occur from millimeters to meters. Organisms capable of adult regeneration offer an intriguing view into this phenomenon, because the regeneration of new tissue involves restoration of relative tissue proportions without transit through embryogenesis and also across these larger length scales.

Freshwater planarians are well known for their ability to regenerate after essentially any injury using neoblast adult pluripotent stem cells [5], but they also undergo robust regulation of proportional growth (Figure 1A). The planarian *Schmidtea mediterranea* grows after feeding and "degrows" after starvation by scaling reversibly over a 40× range in body size from 0.5 to 2 cm in length, largely by regulating total cell numbers from ~1 to 20 million cells [6–8]. Regeneration itself in these animals involves the restoration of proportionality and not initially a restoration of absolute size. After severe body amputations, planarians regenerate missing tissues through a combination of blastema outgrowth to produce new tissue and also the rescaling of preexisting tissue regions, which together produce a smaller but well-proportioned animal over several weeks. The scaling of the planarian head-to-tail anteroposterior (AP) axis is easily accessible to measurement and manipulation for surgery, and regenerated planarians of different sizes attain stereotyped proportions of body features with respect to size (Figure 1B). This biology, combined with genome resources and tools for molecular and functional analysis, has made planarians an emerging model for studying the biology of adult tissue growth and proportionality at the millimeter-to-centimeter scale.

Planarians use a system of nested posterior Wnts and anterior Wnt inhibitors to control tissue identity along the AP axis running from head to tail, which in principle could also regulate AP axis proportionality. Wnt expression, transcriptional interdependence, and functional hierarchy suggest a particular importance of signaling from the axis termini [9–13]. *notum* and *wnt1* are expressed at the anterior and posterior poles and their expression is induced early near amputation sites to control a head-versus-tail decision of the outgrowing blastema through control of canonical Wnt signaling [9–12]. Inhibition of canonical Wnt signaling results in ectopic head regeneration and overactivation results in ectopic tail regeneration [9–18]. However, the distinct contributions of *wnt1* to regeneration through its expression at the posterior pole versus near injury sites, if any, have not yet been resolved. Two other constitutive signaling systems use alternate Wnts and associated factors in order to restrict anterior regionalization along the AP axis: inhibition of *wnt11-6/wntA*, *fzd5/8-4*, or *NDK* results in posterior expansion of the brain and posterior duplication of eyes, *notum* or *prep* inhibition results in anterior duplication of eyes, and *wntP-2/wnt11-5*, *fzd1/2/7*,

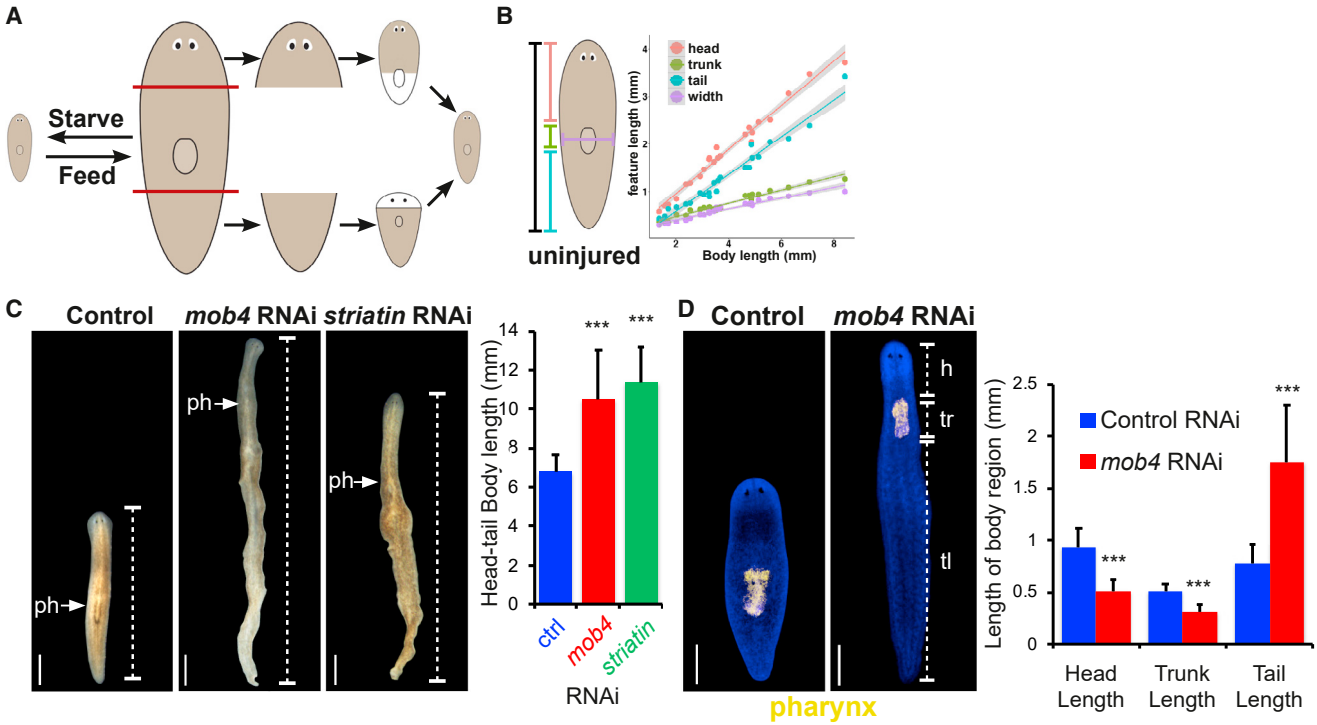

Figure 1. *mob4* Regulates the Ability of Planarians to Proportionally Scale Body Regions

(A) Planarians scale tissue across a 40× size range during homeostasis, and during regeneration rescale existing tissue with newly produced tissue.

(B) The length of different regions of the body (head, trunk, tail, and width) scale proportionally relative to overall body length during homeostasis. Trendlines are linear regressions with 95% confidence intervals calculated in R.

(C) Live images showing long-term homeostatic *mob4(RNAi)* and *striatin(RNAi)* animals have disproportionate body tissue and an anteriorly placed pharynx (ph; arrows). Brackets indicate tail. Graph showing the total length of animals of each RNAi condition. N ≥ 10 animals; error bars are SDs; asterisks denote $p < 0.0005$ by 2-tailed t test.

(D) Fluorescence *in situ* hybridization (FISH) of pharynx progenitor ASXL_059179 to compare the anteroposterior (AP) position of the pharynx of *mob4(RNAi)* animals to controls. Brackets indicate tail (tl), trunk (tr), and head (h) length. Right: the graph shows average head, trunk, and tail length. N = 15 animals; error bars are SDs; asterisks denote $p < 0.0005$ by 2-tailed t test.

Scale bars represent 300 μm.

See also Figure S1.

ptk7, or *ndl-3* inhibition results in posterior duplication of the pharynx [19–21]. Although inhibition of Wnts and associated factors modifies the AP pattern, it is unclear whether the same positional information system underlies proportional axis scaling in general. If so, tissue proportionality could be the result of regulation at the levels of production, propagation, or reception of regionalized signals.

RESULTS

To resolve possible models for planarian proportional scaling, we used RNAi to seek specific phenotypes of aberrant relative body size. We found that long-term inhibition (34 days) of a kinase activator, *mob4* (*phocein*), caused significant changes to proportionality of the planarian body plan resulting in a doubling of the size of the head-to-tail axis, and we verified RNAi knockdown of the *mob4* transcript using qPCR (Figures 1C and S1A–S1D). MOB4 factors are a conserved subfamily of Mob-domain kinase activators that act within the striatin-interacting phosphatase and kinase (STRIPAK) complex to regulate a variety of targets and cellular behaviors [22–24] (Figure S1E). By contrast, other distinct Mob-domain-containing subfamilies include Mob1 factors Mst1/2 that activate NDR/LATS kinases. To determine whether *mob4* likely functioned within a planarian STRIPAK complex, we inhibited *striatin*, the core scaffolding protein of the STRIPAK complex [25]. After 34 days of inhibition, *striatin(RNAi)* animals displayed changes to body size similar to *mob4(RNAi)* (Figure 1C). In addition to overall changes in body size, *mob4(RNAi)* animals had a visibly altered AP axis. Staining for pharynx markers revealed that *mob4(RNAi)* animals underwent a dramatic enlargement of tail tissue, reduction of head and trunk (defined as the length of the region containing the pharynx) regions, and increased length:width ratio (Figures 1D, S1D, and S1F). Compared with controls, *mob4(RNAi)* animals had reduced numbers of *cintillo*+ brain neurons that typically scale to body size [7, 8, 26], indicating a decrease in numbers of anterior cells (Figure S1G). These results suggest that *mob4* could be acting to exclusively restrict posterior tissue, or alternatively could both restrict posterior tissues and promote anterior tissue. To test these possibilities, we compared total *cintillo*+ cell number in untreated animals at day 0 versus animals fed either control double-stranded (ds)RNA or *mob4* dsRNA for

34 days (Figure S1H). We found that compared to untreated animals, control animals increased their *cintillo*+ cell number due to growth after the 34 days of feeding. However, *mob4(RNAi)* animals had no change in total *cintillo*+ cell numbers compared to untreated animals (Figure S1H). Therefore, tail enlargement in *mob4(RNAi)* is accompanied by a failure in anterior growth. Additionally, the ratio of head length to trunk length was unchanged in *mob4(RNAi)* compared to controls (Figure S1I), suggesting that relative proportionality between these tissues is unchanged with respect to each other when *mob4* is inhibited. Finally, *mob4(RNAi)* animals had broadly normal composition of non-regionalized cell types such as neoblasts, epidermal progenitors, muscle, and intestine (Figure S2A). Together, these findings indicate that *mob4* specifically restricts relative and absolute posterior identity and is important for anterior growth.

Positional control genes (PCGs) are signaling molecules expressed in body-wide gradients within body-wall muscle cells that provide cues for body regionalization in planarians [27]. Given the role of *mob4* in regulating body proportionality, we tested the hypothesis that *mob4* inhibition would shift PCG gradients to reflect the new body proportions after *mob4* inhibition. We examined posteriorly expressed Wnt signaling genes *wnt1*, *wnt11-2*, *wnt11-1*, *fz4*, and *wntP-2* and found each domain shifted anteriorly with respect to body length (Figures 2A–2C). By contrast, trunk-expressed *ptk7* and anteriorly expressed *ndl-5* and *sfrp-1* were only slightly restricted compared to total body length, with no statistically significant changes to *ndl-3* or *ndk* (Figures 2A and 2B). However, *mob4* inhibition also had the effect of increasing both the absolute and relative size of the tail, so we further examined whether any posterior PCG expression domains expanded when normalized to tail length. Of these, *wnt1* prominently increased ~10-fold in size into a domain extending beyond the tail, with other posterior PCGs showing smaller increases with respect to tail length (Figure 2C). Furthermore, because *wnt1* is expressed on the dorsal midline, we examined for possible changes to PCGs marking the mediolateral and dorsoventral axes, but these appeared broadly normal after *mob4* inhibition (Figure S2B). Therefore, these analyses pointed to *wnt1* as a primary candidate PCG strongly misregulated in *mob4* RNAi that we hypothesized could mediate some aspects of this phenotype. Indeed, tail-expansion phenotypes arising from inhibition of either *mob4* or *striatin* each corresponded to a dramatic expansion of *wnt1* expression along the midline (Figures 2A and S2C). *wnt1* encodes the most posteriorly expressed Wnt factor and is required for posterior regeneration, but it is unknown whether it is sufficient to drive tail growth [9].

We noted that ectopic *wnt1* expression in *mob4(RNAi)* animals was primarily found within dorsal cells along the midline, similar to normal animals, so we sought to identify markers of putative midline cell types that could undergo regulation of *wnt1* expression. Prior single-cell RNA-seq (sequencing) studies revealed a muscle cell type present along the dorsal midline marked by expression of dd_23400 [28] (Figure 2D). Using double fluorescence *in situ* hybridization (FISH), we found that *wnt1* is exclusively expressed in this subpopulation of muscle cells in untreated animals (112/113 cells counted) and that ectopic *wnt1*+ cells in *mob4(RNAi)* animals also express dd_23400 (190/202 cells counted) (Figure 2D). We next investigated whether *mob4(RNAi)* animals have increased *dd_23400*+ cells. *mob4(RNAi)* animals had normal numbers of *dd_23400*+ cells in the head domain relative to head length as well as normal numbers of total *dd_23400* relative to total body length (Figure S2D). We additionally assessed the expression of *notum*, a Wnt antagonist expressed in the anterior pole and required for regeneration of anterior tissue [11]. However, *mob4* inhibition did not alter the expression of *notum* at the anterior pole, indicating *mob4* likely does not limit *wnt1* at the expense of *notum*+ tissue (Figure S2E). Consistent with this, *notum*+ pole cells did not express *dd_23400.* Together, these results suggest that *mob4* and *striatin* specifically inhibit *wnt1* expression within midline muscle cells outside of the posterior pole, normally limiting the domain of the *wnt1*+ midline posterior pole.

In principle, *mob4* might directly restrict posterior identity and indirectly modify *wnt1* expression, or alternatively *mob4* could restrict *wnt1* expression to in turn control tail regionalization. To distinguish these possibilities, we first asked whether *wnt1* expression changes preceded changes to overall body proportionality after *mob4* inhibition. During short-term inhibition of *mob4* (three dsRNA feedings totaling 10 days or RNAi), *wnt1* expression expansion preceded tail enlargement (Figure 3A). We further tested the interaction of the two genes using double-RNAi experiments. After 3 weeks of inhibition, *mob4(RNAi)* animals had expanded tails, whereas simultaneous inhibition of *wnt1* and *mob4* suppressed the *mob4* tail-expansion phenotype (Figure 3B). We confirmed that *mob4* expression was knocked down in *mob4(RNAi);wnt1(RNAi)* animals (Figure 3C). To determine the specificity of the *mob4-wnt1* relationship, we tested whether inhibition of another posterior PCG, *wntP-2*, could suppress the *mob4* RNAi phenotype. *mob4(RNAi);wntP-2(RNAi)* animals formed elongated tails similar to *mob4(RNAi)* animals, suggesting *mob4* does not act through *wntP-2* (Figure S3A). Using qPCR, we confirmed that *mob4* expression was successfully knocked down in *mob4(RNAi);wntP-2(RNAi)* animals compared to controls (Figure S3B). Posterior Wnts have been reported to undergo cross-regulation for a variety of outputs in the posterior [10, 13, 29], but these results indicate that *mob4* regulation of *wnt1* expression is of particular importance to tail size. In addition, long-term homeostatic inhibition of *wnt1* produced a phenotype effectively opposite of *mob4* RNAi in which tail length was reduced (along with formation of a posterior pharynx), and did not coincide with ectopic posterior expression of trunk (*ndl-3*, *ptk-7*) or anterior (*ndl-5*, *sfrp-1*) markers (Figures S3C and S3D). We conclude that *wnt1* activity is required for *mob4* control of body proportion, and *wnt1* can act as a regulator of posterior size.

Planarians not only actively maintain tissue proportionality during homeostatic maintenance but also undergo substantial rescaling of pre-existing tissues in regeneration after amputation [7, 8], also referred to as morphallaxis or tissue remodeling. Decapitated tail fragments exemplify an extreme case of these transformations as they must reduce the size of the pre-existing posterior, form a new trunk within the old posterior, and grow a head from the amputation site. *mob4(RNAi)* tail fragments failed to undergo posterior reduction and positioned trunk tissue too far anteriorly, indicating the importance of *mob4* for regeneration-induced tissue rescaling (Figure 4A). In addition, *mob4(RNAi)* head fragments failed to form a pharynx, and instead *wnt1* expression extended far into the anterior

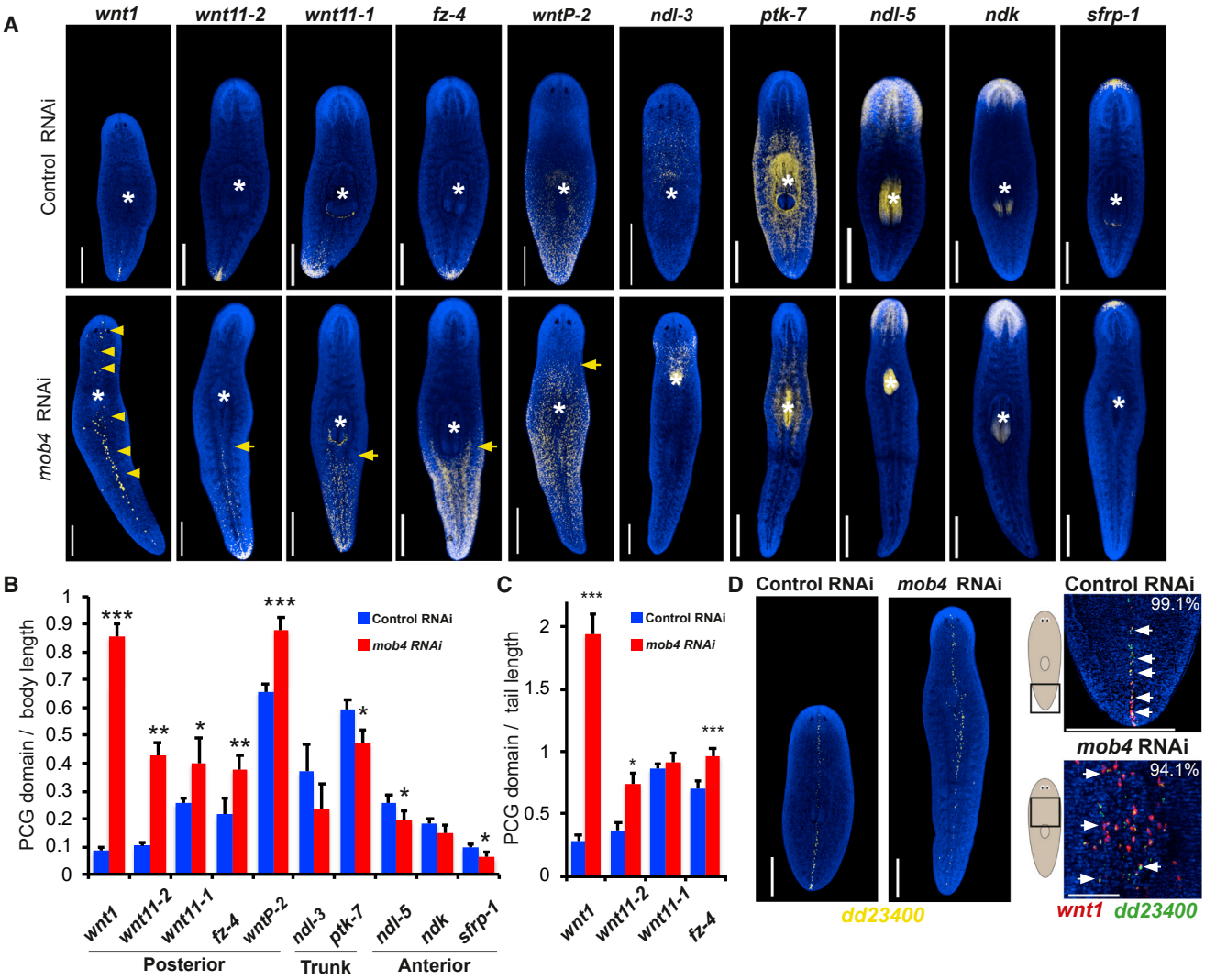

Figure 2. *mob4* Regulates the AP Axis

(A) Animals were fixed after 34 days of *mob4* or control RNAi and stained by FISH as indicated for PCGs marking the AP axis. *mob4* RNAi caused an anterior shift to posterior markers *wnt-1*, *wnt11-2*, *wnt11-1*, *fzd4*, and *wntP-2* and had proportionally slightly reduced expression of trunk markers *ndl-3* and *ptk7* and anterior markers *sfrp-1*, *ndl-5*, and *ndk*. Yellow arrows indicate expanded expression of posterior markers in *mob4(RNAi)* animals. White asterisks indicate pharynx location; n > 4 animals.

(B) Graph showing the length of the indicated PCG domain divided by total length in *mob4(RNAi)* animals compared to controls. *mob4* inhibition had the greatest effect on *wnt1* expression. Error bars are SDs; ***p < 0.0005, **p < 0.005, and *p < 0.05 by 2-tailed t test; n > 4 animals.

(C) Graph showing the length of the indicated PCG domain divided by tail length domain in *mob4(RNAi)* animals compared to controls. *wnt1* is exceptional in the extent of ectopic expression present after *mob4* inhibition. Error bars are SDs; ***p < 0.0005 and *p < 0.05 by 2-tailed t test; n ≥ 4 animals.

(D) Left 2 images: FISH showing *dd23400* expression along the dorsal midline in controls and *mob4(RNAi)*. Right, upper: co-labeling of *wnt1* (red) and *dd23400* (green) showing *wnt1* is exclusively expressed in a population of dorsal midline muscle cells at the posterior pole. Right, lower: *wnt1* expansion in *mob4(RNAi)* animals occurs in dd_23400+ cells.

Scale bars represent 300 μm (A, B, and D, left 2 images) and 150 μm (D, right).

See also Figure S2.

(Figure S4A). Therefore, *mob4* is required for properly defining new posterior territory through the rescaling that occurs during whole-body regeneration.

We further examined the relationship between *wnt1* and *mob4* in regeneration-induced rescaling. Because *wnt1* is necessary for formation of an entirely new posterior end after tail amputation, we examined this relationship in tail fragments that undergo a reduction in posterior territory. Consistent with opposite action with *mob4* in homeostatic maintenance, *wnt1(RNAi)* tail fragments formed their pharynx too far posteriorly, indicating a loss of tail tissue (Figure 4B). In addition to undergoing early wound-site-proximal expression of *wnt1*, we confirmed prior observations that regenerating tail fragments also undergo anterior expansion of *wnt1*'s midline expression (Figure 4C) [9, 12]. Regeneration-induced midline *wnt1* was expressed within dd_23400+ muscle cells, in contrast to wound-proximal *wnt1*

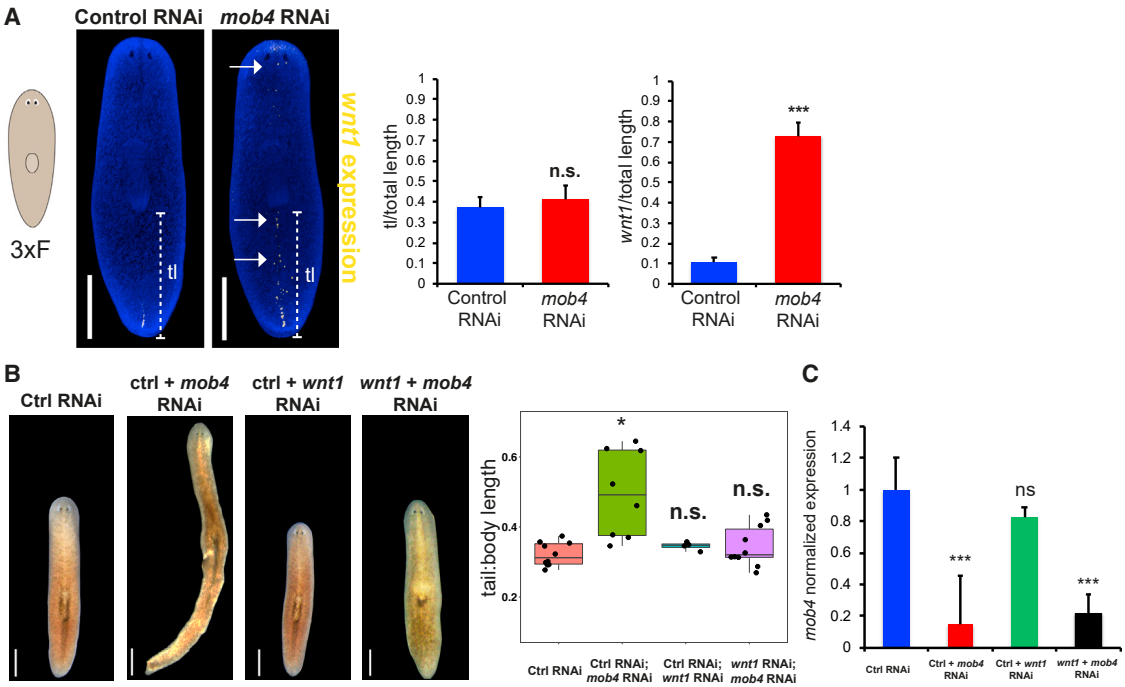

Figure 3. *wnt1* Mediates *mob4* Control of Body Proportionality

(A) FISH to detect *wnt1* showing expanded expression in *mob4(RNAi)* animals (right image) compared to controls (left image) after only 3 dsRNA feedings totaling 10 days of RNAi. Middle: graph showing the tail length divided by total body length. Right: graph showing the length of *wnt1* expression divided by total length. N = 10 animals; error bars are SDs; n.s., not significant, $p > 0.05$ by 2-tailed t test.

(B) Live images showing body morphology of double-RNAi experiments. Compared to controls, *mob4(RNAi)* animals show characteristic body-patterning changes, whereas *wnt1(RNAi)* and *mob4(RNAi);wnt1(RNAi)* animals are unchanged. Right: graph showing the tail length of each RNAi condition. N = 10 animals; error bars are SDs; asterisks denote $p < 0.05$ by 2-tailed t test.

(C) *mob4* mRNA expression measured by qPCR from RNA collected after 17 days of RNAi as indicated. Simultaneous treatment with *wnt1* and *mob4* dsRNA resulted in *mob4* transcript reduction similar to *mob4* dsRNA treatment alone. Error bars are SDs of 4 biological replicates; asterisks denote $p < 0.0005$ by 2-tailed t test. Scale bars represent 300 μm.

See also Figure S3.

expression, and it peaked at 18 h, followed by gradual restriction to the new posterior over time (Figures 4C and 4D). We hypothesized that the rescaling process requires restriction of this domain to the new posterior pole to allow for formation of trunk and head domains, because the *wnt1* expression domain ultimately scales directly with animal length in animals that have completed regeneration (Figure 4E). To test this, we utilized the *mob4(RNAi)* phenotype of *wnt1* pole expansion. In tail fragments following 6 feedings of *mob4* dsRNA, *wnt1* expression was present at the time of wounding (0 h) and was maintained over all times over the course of regeneration (Figure 4C). Under these dsRNA-feeding conditions, 8/12 *mob4(RNAi)* animals regenerate dramatically smaller brains as measured by *cintillo*+ cells and significantly longer tails, whereas 4/12 completely lacked regeneration of any anterior or trunk tissues (Figure S4B). By contrast, control animals underwent *wnt1* midline expansion followed by restriction to allow for proper proportion restoration through regeneration (Figure 4F). Together, these results suggest *wnt1*+ expression at the pole is necessary for posterior proportionality, and *mob4* normally restricts *wnt1*+ pole cells to allow for appropriate anterior and trunk fates.

We next considered the possible mechanisms accounting for *mob4*'s negative regulatory effect on *wnt1* expression. *wnt1* expression could be directly regulated by *mob4* in a signaling event occurring within pre-existing muscle cells, or alternatively by controlling the production of the cells that express *wnt1*. To examine these models, we first considered the expression of *mob4* with respect to midline muscle cells. FISH showed that both *mob4* and *striatin* mRNA were expressed broadly and were not regionally restricted (Figures S5A and S5B), with *mob4* mRNA enriched in the parenchyma. Prior single-cell RNA-seq experiments showed broad and low expression of both genes, with the caveat that low-abundance transcripts may be underrepresented in such datasets (Figures S5A and S5B). Puncta observed from staining with a *mob4* riboprobe were eliminated in *mob4(RNAi)* animals, consistent with low expression of this gene. Because *mob4* expression appeared stronger in the parenchyma, we hypothesized that *mob4* could be expressed in neoblasts or their differentiating progeny and tested this by examining expression in animals treated with lethal doses of X-ray irradiation. This treatment almost completely eliminated expression of *mob4* by 7 days, suggesting that *mob4* expression depends on stem cells or early progenitor cells (Figure 5A). We then used double FISH to determine co-expression of *mob4* and *smedwi-1*, a marker of neoblasts. In confocal slices, we found that *mob4* expression could be detected at

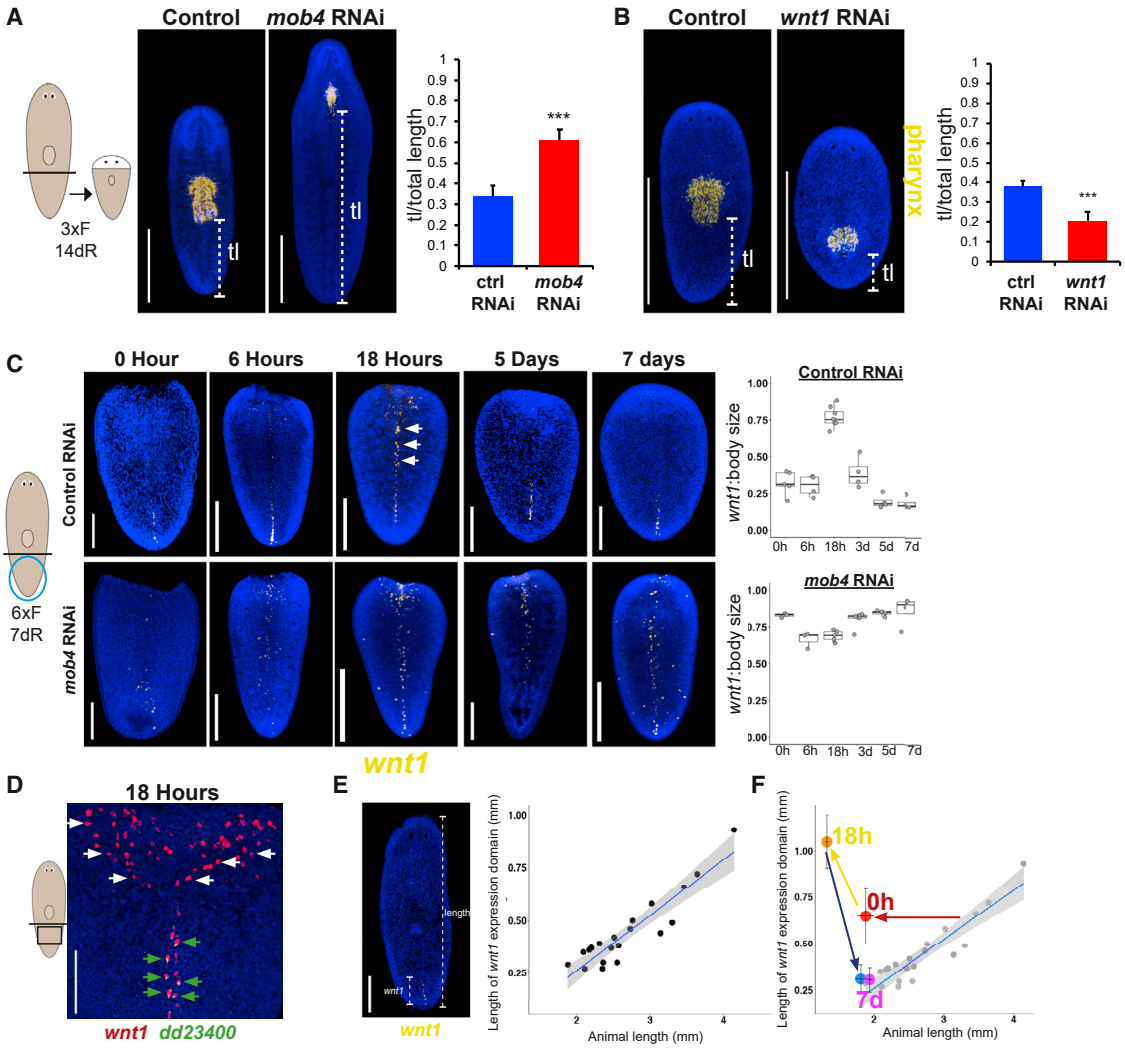

Figure 4. Restriction of *wnt1*+ Midline Cells Controls Rescaling during Regeneration

(A) FISH to detect ASXL_059179 in regenerating tail fragments of controls and *mob4(RNAi)* animals. Animals were fed dsRNA 3 times and regenerated for 14 days. Right: graph showing tail length (brackets) divided by total length of the tail fragment. N > 10 animals; error bars are SDs; asterisks denote $p < 0.0005$ by 2-tailed t test.

(B) FISH detecting ASXL_059179 to measure tail length in regenerating tail fragments in *wnt1(RNAi)* animals compared to controls. Right: graph showing tail length divided by total body length. N = 10 animals; error bars are SDs; asterisks denote $p < 0.0005$ by 2-tailed t test.

(C) Top: FISH showing *wnt1* expression expansion in controls at 18 h after injury along the dorsal midline in tail fragments, followed by a restriction to the posterior tip after 7 days. Arrows indicate expanded *wnt1* expression along the midline at 18 h. Bottom: FISH showing *wnt1* expression in *mob4(RNAi)* animals persists at the dorsal midline throughout regeneration. Animals were fed dsRNA 6 times and regenerated for 7 days. Right: graph showing the quantification of the most anterior midline *wnt1*+ cell outside the region proximal to the wound site divided by total length of the tail fragment in a time series after injury. N > 3 animals for each time point; error bars are SDs.

(D) Double FISH showing *wnt1* (red) is expressed in *dd23400*+ cells (green) in tail fragments 18 h after injury along the dorsal midline, but *wnt1* expression at the wound site is not expressed in *dd23400*+ cells.

(E) FISH to determine the relationship between length of the *wnt1* expression domain versus total length of individual animals (dots). The linear regression line with 95% confidence interval was calculated in R/ggplot2, $R^2 = 0.85$.

(F) Average *wnt1*:body length of regenerating animals from (C) mapped onto uninjured animals from (E).

Scale bars represent 300 μm (A, B, and E) and 150 μm (C and D).

See also Figure S4.

low levels in many but not all neoblasts (Figure S5D). Because neoblasts are 5–10 μm, we used 10-μm maximum projections to quantify co-expression of *mob4* and *smedwi-1* and found that 59.7% of neoblasts had clear *mob4* expression (Figures 5B and S5D). Using similar approaches, we could not detect *mob4* mRNA in either *wnt1*+ posterior pole cells (Figure 5C) or further anterior midline muscle cells (dd_23400+) that do not express *wnt1* (Figure 5D).

These results suggested that *mob4* controls *wnt1* expression and body proportionality through a stem-cell-mediated process

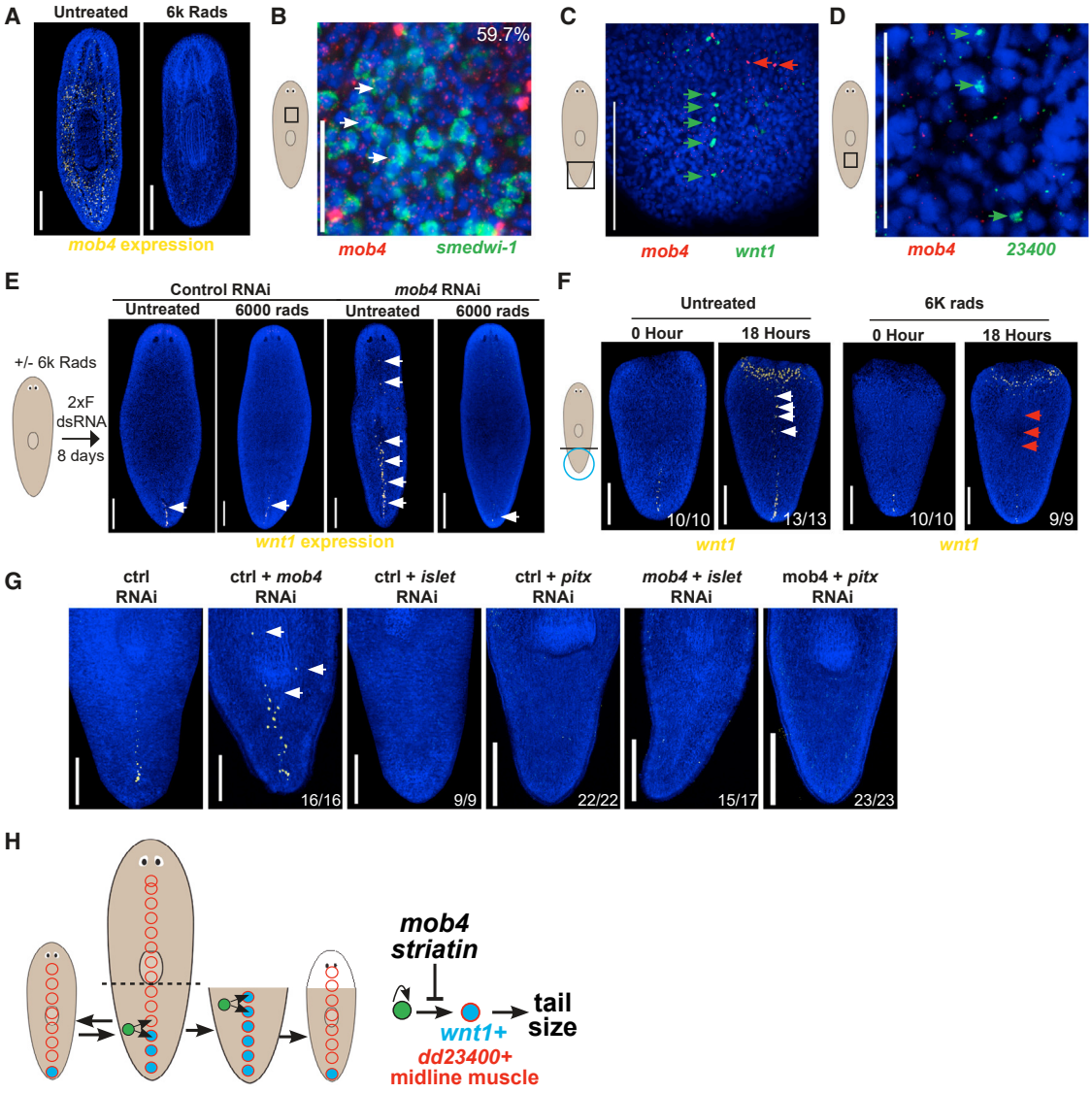

Figure 5. *mob4* Limits Differentiation of Stem Cells into *wnt1*+ Midline Cells

(A) FISH to detect *mob4* showing reduced expression in irradiated animals depleted for stem cells (right) compared to controls (left).

(B) Double FISH of *mob4* (red) and *smedwi-1* (green) showing *mob4* is expressed in 59.7% (242/405) *smedwi-1*+ stem cells.

(C) Double FISH of *mob4* (red) and *wnt1* (green) showing *mob4* is not expressed in *wnt1*+ posterior pole cells.

(D) Double FISH of *mob4* (red) and *dd_23400* (green) showing *mob4* is not expressed in dd_23400+ midline muscle cells.

(E) Left 2 images: FISH showing *wnt1* expression in untreated versus neoblast-depleted irradiated animals after control RNAi feeding. Right 2 images: FISH showing *wnt1* expression in untreated versus neoblast-depleted irradiated animals after *mob4* inhibition.

(F) FISH showing expanded *wnt1* expression along the dorsal midline in tail fragments at 0 or 18 h after injury in untreated animals (left panels) or treated with 6K rad of X-ray irradiation 2 days prior to surgery. N > 5 animals for each time point.

(G) FISH to detect *wnt1* showing expanded expression in *mob4(RNAi)* animals but not in *islet(RNAi)* or *pitx(RNAi)* animals. Double RNAi of *mob4* with either *islet* or *pitx* resulted in the absence of *wnt* expansion.

(H) Model showing stem cells (green) giving rise to either *wnt1*-/*dd23400*+ (red circle) or *wnt1*+/*dd23400*+ pole cells (blue with red border) in the far posterior. *mob4*/*striatin* inhibits the differentiation of *wnt1*+/*dd23400*+ pole cells.

Scale bars represent 300 μm (A, E, and F), 150 μm (B–D), and 300 μm (G).

See also Figure S5.

rather than cell-autonomously within differentiated muscle cells. However, because of the broadness of *mob4* expression, it remained possible that stem cell or progenitor expression of *mob4* was unrelated to control of *wnt1* expression. To examine this possibility, we determined whether *wnt1* expansion after *mob4* RNAi could still occur in animals depleted of neoblasts. Some PCG expression in planarians, including wound-proximal injury-induced *wnt1* expression, can occur in irradiated animals lacking neoblasts, likely because of signaling events occurring only within differentiated cells. We identified the earliest *mob4*

RNAi-dosing conditions resulting in *wnt1* expression expansion (2 feedings encompassing 8 days) and compared this cohort to animals irradiated prior to the same RNAi treatment. Irradiated animals that were fed *mob4* dsRNA failed to undergo *wnt1* expression expansion (Figure 5E). Therefore, neoblasts are required for *mob4*'s effects on *wnt1* expression. Consistent with these results, rescaling-induced *wnt1* expressed along the midline of regenerating tail fragments, but not wound-proximal *wnt1* expression in *dd_23400*− cells, was also eliminated by lethal irradiation (Figure 5F). Based on these results, we reasoned that *mob4* either controls neoblasts in the process of differentiating *wnt1*+ cells or instead might influence *wnt1* expression in pre-existing muscle cells in some process indirectly involving neoblasts. To test these models, we made use of prior work that identified the transcription factors *islet* and *pitx* as required for the production of *wnt1*+ pole cells from neoblasts [30–32]. Inhibition of either *islet* or *pitx* suppressed the *mob4* RNAi phenotype on *wnt1* expression, indicating the effects of *mob4* inhibition require *wnt1*+ cell differentiation. These results suggest that *mob4* primarily acts to inhibit the production of *wnt1*+ cells rather than to repress *wnt1* expression in pre-existing muscle cells (Figure 5G). Using qPCR, we confirmed that *mob4* expression was successfully knocked down in both *mob4(RNAi);islet(RNAi)* and *mob4(RNAi);pitx(RNAi)* animals compared to controls (Figure S5E). Taken together, these results support a model in which *wnt1*+ pole cells determine tail proportionality along the AP axis, with *mob4* controlling *wnt1*+ pole cell numbers through limiting stem-cell-dependent production (Figure 5G).

DISCUSSION

Together, our results indicate that STRIPAK suppression of Wnt signaling is a critical pathway regulating whole-body proportional scaling in planarians. STRIPAK complexes regulate a variety of processes including cell growth, differentiation, signaling, proliferation, apoptosis, and tumorigenesis, using a variety of inputs [24]. In planarians, the activity of a separate *striatin* gene was possibly needed for the functioning of neoblast progeny [33]. Recently, multiple studies have identified STRIPAK as a key negative regulator of Hippo signaling [34, 35], although planarian Hippo pathway components do not obviously function in AP tissue proportionality. Hippo RNAi results in modifications to proliferation, decreased cell death, and formation of undifferentiated lesions, whereas *yorkie(RNAi)* animals have elevated injury-induced *wnt1* as well as regeneration failure and excretory cell dysfunction [36–38]. Additionally, *yorkie(RNAi)* animals have both ectopic *wnt1* and *notum* cells during homeostasis, but without obvious changes to the position of tissues along the AP axis. We hypothesize that the pleiotropic roles of *yorkie* may mask specific contributions to tail size via *wnt1* expression regulation. Our results raise the possibility that STRIPAK could exert context-specific regulation of Yorkie functions.

wnt1 is a multifunctional factor in planarian regeneration. Inhibition of wound-induced *follistatin* results in excess wound-proximal, injury-induced *wnt1* expression leading to the failure of head regeneration [39]. In addition, RNAi of *wnt1* only after injury in head fragments caused ectopic head regeneration, indicating its effects on axis polarization are injury induced [10]. By contrast, in regenerating animals, pole expression of *wnt1* is impaired in irradiated animals or after inhibition of several transcription factors: *Djislet*, *junli*, and *pitx* [10, 30–32, 40]. How *wnt1* may act upstream of or in parallel to other posteriorly expressed factors for tail specification and sizing has not yet been resolved. However, the *mob4(RNAi)* phenotype does not involve an inversion of axis polarization, indicating the independence between tissue polarity and body regionalization used for tissue proportionality in regeneration.

Planarians scale all body regions with respect to each other and across all body axes. Factors responsible for overall animal growth could include pathways responsive to nutrient status and link to generalized control of neoblast differentiation rates. By contrast, proportional scaling involves controlling the relative sizes of local regions with respect to each other. Here we implicate *mob4* and the STRIPAK complex in scaling tail size with respect to body size via regulation of *wnt1.* Homeostatic *wnt1*-dependent tail enlargement in *mob4(RNAi)* coincided with a lack of anterior growth, suggesting that at least some aspects of the planarian tissue-scaling system could be mediated through individual control of discrete body regions. These findings raise the possibility that planarian positional control genes expressed from muscle might in general function both in regional identity determination and also in regional proportional scaling. Because these genes are constitutively expressed in the absence of injury, the reattainment of normal proportions across the body through regeneration might then involve a process that achieves a stable equilibrium of these local signaling processes across all body regions.

In principle, the determinants of axis scale could be regulated through signaling across fields of existing cells, either by ensembles of cells controlled locally through junctional signals or directed by morphogens acting at a distance. Our results indicate the importance of generating the cells that produce a secreted factor, *wnt1*, at an axis boundary in order to control the regional proportionality along that body axis. Signaling through planarian stem cells is necessary for production of the *notum*+ anterior pole and both to produce [41–44] and limit the production of the *wnt1*+ posterior pole. Therefore, regulating the production of signaling-center cells through stem cell differentiation could be a critical component of establishing proportional scaling in regeneration.

STAR★METHODS

Detailed methods are provided in the online version of this paper and include the following:

- KEY RESOURCES TABLE
- LEAD CONTACT AND MATERIALS AVAILABILITY
- EXPERIMENTAL MODEL AND SUBJECT DETAILS
- METHOD DETAILS
  - Fluorescent *in situ* hybridization (FISH)
  - RNAi administration
  - Image Acquisition and Quantification
  - Body Length Measurements
  - Cell Counting
- QUANTIFICATION AND STATISTICAL ANALYSIS
- DATA CODE AND AVAILABILITY

SUPPLEMENTAL INFORMATION

Supplemental Information can be found online at https://doi.org/10.1016/j.cub.2019.11.068.

ACKNOWLEDGMENTS

We thank members of the Petersen lab and Dr. Eric Hill for critical comments. C.P.P. acknowledges funding from the National Institutes of Health, USA (NIGMS R01GM129339 and R01GM130835), and pilot project funding from the NSF-Simons Center for Quantitative Biology at Northwestern University, an NSF (1764421)-Simons/SFARI (597491-RWC) MathBioSys Research Center.

AUTHOR CONTRIBUTIONS

C.P.P. conceived of the study and acquired funding, E.G.S. designed and conducted experiments, and C.P.P. and E.G.S. wrote the manuscript.

DECLARATION OF INTERESTS

The authors declare no competing interests.

Received: June 3, 2019
Revised: October 14, 2019
Accepted: November 22, 2019
Published: January 9, 2020

REFERENCES

1. Thompson, D.W. (1942). On Growth and Form (Cambridge University Press).
2. Hariharan, I.K. (2015). Organ size control: lessons from *Drosophila*. Dev. Cell *34*, 255–265.
3. Kicheva, A., and Briscoe, J. (2015). Developmental pattern formation in phases. Trends Cell Biol. *25*, 579–591.
4. Schwank, G., and Basler, K. (2010). Regulation of organ growth by morphogen gradients. Cold Spring Harb. Perspect. Biol. *2*, a001669.
5. Wagner, D.E., Wang, I.E., and Reddien, P.W. (2011). Clonogenic neoblasts are pluripotent adult stem cells that underlie planarian regeneration. Science *332*, 811–816.
6. Baguñà, J., Romero, R., Saló, E., Collet, J., Carme, A., Ribas, M., Riutort, M., García-Fernàndez, J., Burgaya, F., and Bueno, D. (1990). Growth, degrowth and regeneration as developmental phenoma in adult freshwater planarians. In Experimental Embryology in Aquatic Plants and Animals, *Volume 195*, H.J. Marthy, ed. (Springer), pp. 129–162.
7. Hill, E.M., and Petersen, C.P. (2015). Wnt/Notum spatial feedback inhibition controls neoblast differentiation to regulate reversible growth of the planarian brain. Development *142*, 4217–4229.
8. Oviedo, N.J., Newmark, P.A., and Sánchez Alvarado, A. (2003). Allometric scaling and proportion regulation in the freshwater planarian *Schmidtea mediterranea*. Dev. Dyn. *226*, 326–333.
9. Petersen, C.P., and Reddien, P.W. (2008). Smed-betacatenin-1 is required for anteroposterior blastema polarity in planarian regeneration. Science *319*, 327–330.
10. Petersen, C.P., and Reddien, P.W. (2009). A wound-induced Wnt expression program controls planarian regeneration polarity. Proc. Natl. Acad. Sci. USA *106*, 17061–17066.
11. Petersen, C.P., and Reddien, P.W. (2011). Polarized notum activation at wounds inhibits Wnt function to promote planarian head regeneration. Science *332*, 852–855.
12. Gurley, K.A., Elliott, S.A., Simakov, O., Schmidt, H.A., Holstein, T.W., and Sánchez Alvarado, A. (2010). Expression of secreted Wnt pathway components reveals unexpected complexity of the planarian amputation response. Dev. Biol. *347*, 24–39.
13. Stückemann, T., Cleland, J.P., Werner, S., Thi-Kim Vu, H., Bayersdorf, R., Liu, S.Y., Friedrich, B., Jülicher, F., and Rink, J.C. (2017). Antagonistic self-organizing patterning systems control maintenance and regeneration of the anteroposterior axis in planarians. Dev. Cell *40*, 248–263.e4.
14. Gurley, K.A., Rink, J.C., and Sánchez Alvarado, A. (2008). Beta-catenin defines head versus tail identity during planarian regeneration and homeostasis. Science *319*, 323–327.
15. Iglesias, M., Gomez-Skarmeta, J.L., Saló, E., and Adell, T. (2008). Silencing of Smed-betacatenin1 generates radial-like hypercephalized planarians. Development *135*, 1215–1221.
16. Owen, J.H., Wagner, D.E., Chen, C.C., Petersen, C.P., and Reddien, P.W. (2015). teashirt is required for head-versus-tail regeneration polarity in planarians. Development *142*, 1062–1072.
17. Reuter, H., März, M., Vogg, M.C., Eccles, D., Grífol-Boldú, L., Wehner, D., Owlarn, S., Adell, T., Weidinger, G., and Bartscherer, K. (2015). β-catenin-dependent control of positional information along the AP body axis in planarians involves a teashirt family member. Cell Rep. *10*, 253–265.
18. Beane, W.S., Morokuma, J., Lemire, J.M., and Levin, M. (2013). Bioelectric signaling regulates head and organ size during planarian regeneration. Development *140*, 313–322.
19. Felix, D.A., and Aboobaker, A.A. (2010). The TALE class homeobox gene Smed-prep defines the anterior compartment for head regeneration. PLoS Genet. *6*, e1000915.
20. Lander, R., and Petersen, C.P. (2016). Wnt, Ptk7, and FGFRL expression gradients control trunk positional identity in planarian regeneration. eLife *5*, e12850.
21. Scimone, M.L., Cote, L.E., Rogers, T., and Reddien, P.W. (2016). Two FGFRL-Wnt circuits organize the planarian anteroposterior axis. eLife *5*, e12845.
22. Baillat, G., Moqrich, A., Castets, F., Baude, A., Bailly, Y., Benmerah, A., and Monneron, A. (2001). Molecular cloning and characterization of phocein, a protein found from the Golgi complex to dendritic spines. Mol. Biol. Cell *12*, 663–673.
23. Moreno, C.S., Lane, W.S., and Pallas, D.C. (2001). A mammalian homolog of yeast MOB1 is both a member and a putative substrate of striatin family-protein phosphatase 2A complexes. J. Biol. Chem. *276*, 24253–24260.
24. Shi, Z., Jiao, S., and Zhou, Z. (2016). STRIPAK complexes in cell signaling and cancer. Oncogene *35*, 4549–4557.
25. Moreno, C.S., Park, S., Nelson, K., Ashby, D., Hubalek, F., Lane, W.S., and Pallas, D.C. (2000). WD40 repeat proteins striatin and S/G(2) nuclear autoantigen are members of a novel family of calmodulin-binding proteins that associate with protein phosphatase 2A. J. Biol. Chem. *275*, 5257–5263.
26. Takeda, H., Nishimura, K., and Agata, K. (2009). Planarians maintain a constant ratio of different cell types during changes in body size by using the stem cell system. Zool. Sci. *26*, 805–813.
27. Witchley, J.N., Mayer, M., Wagner, D.E., Owen, J.H., and Reddien, P.W. (2013). Muscle cells provide instructions for planarian regeneration. Cell Rep. *4*, 633–641.
28. Fincher, C.T., Wurtzel, O., de Hoog, T., Kravarik, K.M., and Reddien, P.W. (2018). Cell type transcriptome atlas for the planarian *Schmidtea mediterranea*. Science *360*, eaaq1736.
29. Sureda-Gómez, M., Pascual-Carreras, E., and Adell, T. (2015). Posterior Wnts have distinct roles in specification and patterning of the planarian posterior region. Int. J. Mol. Sci. *16*, 26543–26554.
30. Currie, K.W., and Pearson, B.J. (2013). Transcription factors lhx1/5-1 and pitx are required for the maintenance and regeneration of serotonergic neurons in planarians. Development *140*, 3577–3588.
31. Hayashi, T., Motoishi, M., Yazawa, S., Itomi, K., Tanegashima, C., Nishimura, O., Agata, K., and Tarui, H. (2011). A LIM-homeobox gene is required for differentiation of Wnt-expressing cells at the posterior end of the planarian body. Development *138*, 3679–3688.
32. März, M., Seebeck, F., and Bartscherer, K. (2013). A Pitx transcription factor controls the establishment and maintenance of the serotonergic lineage in planarians. Development *140*, 4499–4509.

33. Reddien, P.W., Bermange, A.L., Murfitt, K.J., Jennings, J.R., and Sánchez Alvarado, A. (2005). Identification of genes needed for regeneration, stem cell function, and tissue homeostasis by systematic gene perturbation in planaria. Dev. Cell *8*, 635–649.

34. Chen, M., Zhang, H., Shi, Z., Li, Y., Zhang, X., Gao, Z., Zhou, L., Ma, J., Xu, Q., Guan, J., et al. (2018). The MST4-MOB4 complex disrupts the MST1-MOB1 complex in the Hippo-YAP pathway and plays a pro-oncogenic role in pancreatic cancer. J. Biol. Chem. *293*, 14455–14469.

35. Zheng, Y., Liu, B., Wang, L., Lei, H., Pulgar Prieto, K.D., and Pan, D. (2017). Homeostatic control of Hpo/MST kinase activity through autophosphorylation-dependent recruitment of the STRIPAK PP2A phosphatase complex. Cell Rep. *21*, 3612–3623.

36. de Sousa, N., Rodríguez-Esteban, G., Rojo-Laguna, J.I., Saló, E., and Adell, T. (2018). Hippo signaling controls cell cycle and restricts cell plasticity in planarians. PLoS Biol. *16*, e2002399.

37. Lin, A.Y., and Pearson, B.J. (2014). Planarian yorkie/YAP functions to integrate adult stem cell proliferation, organ homeostasis and maintenance of axial patterning. Development *141*, 1197–1208.

38. Lin, A.Y.T., and Pearson, B.J. (2017). Yorkie is required to restrict the injury responses in planarians. PLoS Genet. *13*, e1006874.

39. Tewari, A.G., Stern, S.R., Oderberg, I.M., and Reddien, P.W. (2018). Cellular and molecular responses unique to major injury are dispensable for planarian regeneration. Cell Rep. *25*, 2577–2590.e3.

40. Tejada-Romero, B., Carter, J.M., Mihaylova, Y., Neumann, B., and Aboobaker, A.A. (2015). JNK signalling is necessary for a Wnt- and stem cell-dependent regeneration programme. Development *142*, 2413–2424.

41. Chen, C.C., Wang, I.E., and Reddien, P.W. (2013). pbx is required for pole and eye regeneration in planarians. Development *140*, 719–729.

42. Scimone, M.L., Lapan, S.W., and Reddien, P.W. (2014). A forkhead transcription factor is wound-induced at the planarian midline and required for anterior pole regeneration. PLoS Genet. *10*, e1003999.

43. Vásquez-Doorman, C., and Petersen, C.P. (2014). zic-1 expression in planarian neoblasts after injury controls anterior pole regeneration. PLoS Genet. *10*, e1004452.

44. Vogg, M.C., Owlarn, S., Pérez Rico, Y.A., Xie, J., Suzuki, Y., Gentile, L., Wu, W., and Bartscherer, K. (2014). Stem cell-dependent formation of a functional anterior regeneration pole in planarians requires Zic and Forkhead transcription factors. Dev. Biol. *390*, 136–148.

45. Pearson, B.J., Eisenhoffer, G.T., Gurley, K.A., Rink, J.C., Miller, D.E., and Sánchez Alvarado, A. (2009). Formaldehyde-based whole-mount in situ hybridization method for planarians. Dev. Dyn. *238*, 443–450.

46. King, R.S., and Newmark, P.A. (2013). In situ hybridization protocol for enhanced detection of gene expression in the planarian *Schmidtea mediterranea*. BMC Dev. Biol. *13*, 8.

47. Rouhana, L., Weiss, J.A., Forsthoefel, D.J., Lee, H., King, R.S., Inoue, T., Shibata, N., Agata, K., and Newmark, P.A. (2013). RNA interference by feeding in vitro-synthesized double-stranded RNA to planarians: methodology and dynamics. Dev. Dyn. *242*, 718–730.

STAR★METHODS

KEY RESOURCES TABLE

REAGENT or RESOURCE	SOURCE	IDENTIFIER
Antibodies		
anti-digoxigenin-POD, Fab fragments	Sigma/Roche	# 11207733910
		RRID: AB_514500
anti-fluorescein-POD, Fab fragments	Sigma/Roche	#11426346910
		RRID: AB_840257
Experimental Models: Organisms/Strains		
Schmidtea mediterranea, clonal strain CIW4, asexual	Laboratory of Christian Petersen	N/A
Freshwater medium for rearing planarians: 1x Montjuic salts (1.6 mmol/l NaCl, 1.0 mmol/l CaCl2, 1.0 mmol/l MgSO4, 0.1 mmol/l MgCl2, 0.1 mmol/l KCl and 1.2 mmol/l NaHCO3 in Milli-Q water, pH 6.9-8.1)	Laboratory of Christian Petersen	N/A
Oligonucleotides		
See Table S1 for the list of DNA oligos	Integrated DNA Technologies	N/A
Software and Algorithms		
ImageJ (FIJI)		https://fiji.sc
Metamorph	Molecular Devices	https://www.moleculardevices.com/products/cellular-imaging-systems/acquisition-and-analysis-software/metamorph-microscopy#gref
Leica LAS	Leica	https://www.leica-microsystems.com/products/microscope-software/p/leica-las-x-ls/
R Studio	R Studio	https://rstudio.com/

LEAD CONTACT AND MATERIALS AVAILABILITY

Further information and requests for reagents may be directed to, and will be fulfilled by, the Lead Contact, Dr. Christian Petersen, christian-p-petersen@northwestern.edu. All unique/stable reagents generated in this study are available from the lead contact without restriction.

EXPERIMENTAL MODEL AND SUBJECT DETAILS

Asexual Schmidtea mediterranea animals (CIW4 strain) were maintained in 1x Montjuic salts (1.6 mmol/l NaCl, 1.0 mmol/l CaCl2, 1.0 mmol/l MgSO4, 0.1 mmol/l MgCl2, 0.1 mmol/l KCl and 1.2 mmol/l NaHCO3 in Milli-Q water, pH 6.9-8.1) between 18–20°C. Animals were fed a puree of calf liver (Western Veal Liver Non-Formula Feed product #2180 from Golden Gate Meat Co., 550 Seventh Street, San Francisco CA 94103), homogenized using a Juiceman JM400 Electric Juicer after removal of the casing and stored at −80 in aliquots. Animals were starved for at least 5 days before experiments.

METHOD DETAILS

Fluorescent *in situ* hybridization (FISH)

Animals were killed in 5% NAC in PBS, fixed in 4% formaldehyde and bleached in 6% H2O2 in either Methanol or PBS as described previously [45, 46]. Riboprobes (digoxigenin- or fluorescein-labeled) were synthesized by *in vitro* transcription [45, 46] using PCR templates amplified to contain T7 RNA binding sites for antisense transcription. Anti-Digoxigenin-POD or Anti-Fluorescein-POD Antibodies were used in TNTx/10% horse serum/10% Western Blocking Reagent (Roche, Basel Switzerland) at a concentration of 1:2000 for anti-DIG-POD (Roche, Basel Switzerland), and 1:2000 for anti-FL-POD (Roche). For multiplex FISH, peroxidase conjugated enzyme activity was quenched between tyramide reactions by sodium azide treatment (100 mM in 1xPBSTx) for 45 min at room temperature. Nuclear counterstaining was performed using Hoechst 33342 (Invitrogen, 1:1000 in 1xPBSTx). Primers for probe design are indicated in Table S1.

RNAi administration

dsRNA was generated by T7 *in vitro* transcription of PCR templates to generate sense and antisense transcripts, Ethanol precipitated, annealed at 72 degrees, and verified by gel electrophoresis. RNAi feeding was performed from *in vitro* transcribed dsRNA mixed with 80% liver paste and 5% red food dye [47]. In all RNAi experiments animals were fed RNAi food every 2–3 days for the length of experiment indicated. Figures 1C, 1D, 2D, 3B, S1D, S1F–S1I, S2, and S3A–S3C are homeostatic animals fed 12 times or for 34 days of RNAi. Figures 2A–2C are homeostatic animals fed 9 times or a total of 26 days RNAi. Figure S3D are homeostatic animals fed 10 times or a total of 28 days RNAi. Figures 5G and S5F are homeostatic animals were fed 6 times for a total of 19 days of RNAi. Figure S5C are homeostatic animals fed 4 times or a total of 12 days of RNAi. Figures 4A, 4B, and S4A are regenerating animals fed 3 times, while Figures 4C and S4B are regenerating animals fed 6 times. Primers for RNAi are indicated in Table S1.

Image Acquisition and Quantification

Live images of animals were performed with a Leica M210F dissecting microscope scope with a Leica DFC295 camera. FISH images were performed a Leica DM5500B compound microscope with optical sectioning by Optigrid structured illumination or a Leica SP5 or Leica TCS SPE confocal compound microscopes. Fluorescent images collected by compound microscopy are maximum projections of a z stack and adjusted for brightness and contrast using Metamorph, Adobe Photoshop, or Fiji/ImageJ.

Body Length Measurements

Total animal and regional lengths were measured with Metamorph as visualized with Hoechst or the pharynx progenitor marker asxl_059179. Changes to tissue domain lengths during homeostasis were assessed following at least 34 days of RNAi feeding. Changes to tissue domain lengths during regeneration were assessed following at least 10 days of RNAi feeding. Domain lengths were averaged and significant differences determined by two-tailed Student's t tests. Quantification in Figure 4C is the length of the most anterior midline *wnt1+* cell outside the region 200 microns proximal to the wound site divided by the total body length. Significant differences determined by two-tailed Student's t tests.

Cell Counting

In Figure S1D, *cto+* cells were imaged using a Leica DM5500B compound microscope with optical sectioning equipped with an Optigrid structured illumination device. After a maximum projection of z stacks, *cto+* cells were counted manually in Metamorph. *cto+* cell numbers were averaged and significance was determined by two-tailed t tests. In Figures 5B and S5C using a Leica TCS SPE confocal microscope, we took a 10uM projection of *mob4* and *smedwi-1* expression to ensure that *mob4* expression was in the same plane as neoblasts, which are 5-10 μm in size. Double positive cells were counted manually from 5 separate worms Leica LAS software.

QUANTIFICATION AND STATISTICAL ANALYSIS

Statistical analyses were performed in Microsoft Excel unless indicated otherwise. Statistical tests, significance, data points, error bars, replicates, and other information relevant to figures are described and explained in corresponding legends. Experiments were conducted with at least 5 animals per condition unless otherwise noted. No specific strategy was employed for randomization, blinding, sample-size estimation, or testing normality. No subjects or data were excluded from analysis.

DATA CODE AND AVAILABILITY

This study did not generate any unique datasets or code.